

## Development Status of Lead-bismuth-cooled Fast Reactor for Marine Application

Tung D. C. Nguyen<sup>a</sup>, Muhammad F. Khandaq<sup>a</sup>, Eun Jeong<sup>a</sup>, Jiwon Choe<sup>a</sup>, Kiho Kim<sup>b</sup>, Douglas A. Fynan<sup>a</sup>, Deokjung Lee<sup>a\*</sup>

<sup>a</sup>Ulsan National Institute of Science and Technology (UNIST), 50 UNIST-gil, Ulsan 44919, Republic of Korea

<sup>b</sup>Korea Institute of Nuclear Safety, 62 Gwahak-ro, Yuseong-gu, Daejeon 34142, Republic of Korea

\*Corresponding author: deokjung@unist.ac.kr

### 1. Introduction

This paper presents the core design for MicroURANUS which is a long-cycle lead-bismuth-cooled fast reactor for marine applications. MicroURANUS can be deployed on floating power plants, merchant ships, or icebreakers in single reactor or clustered configurations. MicroURANUS evolved from the URANUS project with numerous modifications introduced to the core geometry, reactor materials, and operational characteristics to satisfy marine-propulsion-specific design objectives and constraints and to achieve long-cycle operation. The reference marine application is icebreaker propulsion with assumed hull life of 40 years and 75% capacity factor giving 30 effective full-power years (EFPYs) at 60 MW<sub>th</sub> nominal power. Most merchant ships are scrapped between 20 to 30 years of age dependent market conditions, so the icebreaker metrics bound the marine-propulsion application space. To de-risk the near-term deployment of MicroURANUS, uranium oxide fuel (UO<sub>2</sub>) was selected considering the mature operational base for UO<sub>2</sub> in commercial light and heavy water reactors and some LMFRs and domestic fuel manufacturing infrastructure in Korea.

### 2. Computer Codes

Two radiation transport codes were used for the MicroURANUS core design: the deterministic Argonne Reactor Computation (ARC) code system [1] and the Monte Carlo (MC) code MCS [2].

ARC [1] is a code package for fast reactor analysis developed by ANL, which includes three main modules: (i) a multigroup cross-section generation code (MC2-3) that generates problem-dependent ultrafine-group (UFG) cross-sections (XSs); (ii) TWODANT, which produces UFG fluxes derived from the Boltzmann transport equation using the discrete ordinate method; and (iii) REBUS-3, which performs nodal diffusion or transport and depletion calculations for fast reactor fuel analyses.

MCS is a 3D continuous-energy neutron-physics code for particle transport based on the MC method, under development at UNIST since 2013 [2]. MCS can conduct criticality runs for reactivity calculations and fixed source runs for shielding problems. MCS has been designed from scratch since 2013 to conduct whole-core criticality simulations with pin-wise depletion and thermal/hydraulic feedback.

### 3. Design Objectives and Constraints

Table I summarizes the technological, material, and regulatory constraints and performance objectives for the MicroURANUS core with assumed 60 MW<sub>th</sub>/20 MW<sub>e</sub> power output for 30 EFPY. As a SMR design for maritime propulsion without refueling target application, MicroURANUS is envisioned to be fully assembled in a factory, analyzed, and then transported to and installed in the ship. During the ship decommissioning, the reactor would be removed (as a single unit without removing spent fuel from the primary vessel) and transported to either long-term waste storage/geological disposal or an international fuel reprocessing facility. The principal size constraints on the core, internal structures, and primary vessel are imposed by capacity of commercial transportation casks licensed for spent nuclear fuel. The suggested canister cavity size of the cask should not exceed the maximum inner diameter and length of 2.4 and 9.2 m, respectively, reflecting manufacturing capability and integrated construction weight. Excessive construction weight which scales nonlinearly with increasing diameter is an issue during both the cask manufacturing process and heavy lifts during loading, transportation, and offloading. Therefore, the reactor vessel of MicroURANUS should be designed with an outer diameter of less than 2.4 m. Any reduction in reactor diameter should be prioritized whereas the reactor height is less constrained.

The MicroURANUS fuel design predicated a low fuel power density an order of magnitude lower than conventional LMFR fuel to achieve the long cycle. Low fuel operating temperature is an inherent property of MicroURANUS implying huge thermal margins with respect to safety limits. Fuel temperature is a degree-of-freedom which can be tuned to obtain other performance objectives including less than 1\$ excess reactivity from hot-zero power (HZIP) to hot-full power (HFP) and practical elimination of core melt/severe accidents.

Fast-spectrum core concepts utilizing liquid lead or lead-bismuth eutectic (LBE) coolants have the favorable characteristics of low-pressure operation, natural circulation capability, gamma-shielding properties, low melting point (for LBE), high boiling point, and chemical stability with water and air [3]. The Ti-stabilized austenitic stainless steel 15-15Ti was selected as the cladding material, because of its outstanding thermal conductivity, irradiation resistance, and superior swelling resistance compared to other alloys [4].

The maximum-allowed fuel enrichment is set to the 19.75% <sup>235</sup>U, the low-enriched uranium (LEU), corresponding to restriction on uranium enrichment for

civilian use. All enrichment zones in this study must not exceed the enrichment of 19.75%. The inlet coolant temperature in the primary loop is chosen, accounting for the properties of the typical austenitic steel in contact with LBE and driven by an electromagnetic pump system to sustain the desired outlet temperature.

Based on the selection of the primary design parameters and the technological and safety constraints, the optimization of the core, fuel design, and loading patterns will be performed to satisfy all the design requirements and to enhance the economic efficiency and safety of MicroURANUS.

Table I: Material-related Technological Constraints and Performance Targets

Parameter	Value
Fuel	UO <sub>2</sub>
- Smear density, %TD*	95
- Maximum <sup>235</sup> U enrichment, %	< 19.75
Coolant	LBE
- Inlet/outlet temperature, °C	250/350
- Pressure, MPa	0.1
Maximum reactor diameter, m	2.40
Change in reactivity (HZP → HFP), \$	< 1
Burnup reactivity swing, \$	< 1

\*Theoretical Density

#### 4. Design Strategy of the Conceptual Core

The assembly design parameters are shown in Table II. The pin diameter was selected as 2.0 cm with a P/D ratio of 1.08, yielding a 0.16 cm gap between two adjacent fuel pins. The hexagonal fuel assembly (FA) geometry shown in Fig. 1 is 61 fuel pins arranged on the hexagonal lattice.

Table II: Design Parameters for MicroURANUS Assembly.

Parameters	Value
Pin data	
- Pin diameter, cm	2.0
- Helium gap size, cm	0.015
- Cladding thickness, cm	0.095
- Pin pitch, cm	2.16
- Pin pitch-to-diameter ratio	1.08
Assembly data	
- Number of pins	61
- Assembly pitch, cm	17.15
Volume fraction at manufacture, %	
- Fuel or absorber	59.59
- Helium gap	2.03
- Structure	13.62

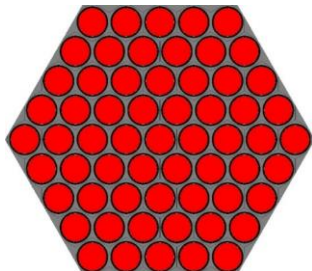


Fig. 1. Fuel assembly design geometry.

Three types of enrichment zoning, Type I, II, and III, are considered in this study, as shown in Fig. 2. These three types have the same active core size; however, Type I is a uniform enrichment zone, whereas Type II and Type III have two enrichment zones, an inner zone and outer zone. Type III is distinguished from TYPE II by additionally introducing axial zoning (25 cm at the top and bottom of the fuel rod), namely onion zoning. The main parameters for each layout type are summarized in Table III. The optimization is conducted with a 60°, 1/6th symmetric core model using the deterministic code system ARC. All material compositions were homogenized assembly-wise based on volume fractions. The MG XS library ENDF/B-VII.0 was used. For the burnup calculations, the burnup step interval was set to 1 year representing 2.5% of the target 40 EFPY burnup.

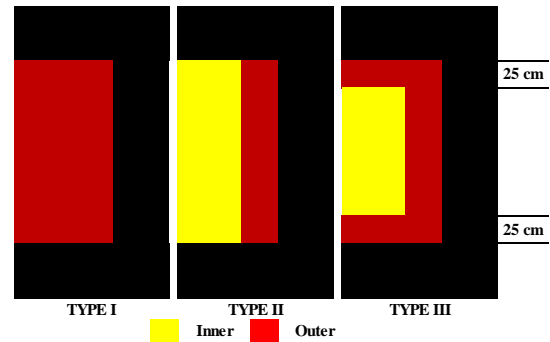


Fig. 2. Fuel arrangement for three core candidates.

Table III. Core Parameters of the Three Core Candidates.

Parameters	Type I	Type II	Type III
Enrichment zones	1	2	2
U <sup>235</sup> enrichment, %	11.5	10.0/13.5	10.0/13.5
Axial zoning, cm	--	--	25
# inner/outer/total FAs	--/--/85	37/48/85	37/48/85
Avg. U <sup>235</sup> enrichment, %	11.5	12.0	12.5

Fig. 3 illustrates the behaviors of  $k_{eff}$  and the conversion ratio over time, showing that all three core candidates can achieve a lifetime over 30 EFPYs. The average <sup>235</sup>U enrichment of each type is 11.5%, 12.0% and 12.5%, respectively. The 2D R-Z power profiles (normalized so that the average power equals 1.0 over the active core region) at the beginning of cycle (BOC), middle-of-cycle (MOC, t = 20 EFPY), and end-of-cycle (EOC, t = 40 EFPY) for the three core candidates are as shown in Fig. 4. The Type I core has the largest fertile <sup>238</sup>U inventory and as a uniform cylinder geometry, the most centered-peaked power distribution with power peaking factor of approximately 1.80. This low-leakage design results in the highest conversion ratio (see Fig. 4b). The zoned-enrichment strategies of Type II and III flatten the power distribution. Superior flattening is achieved with onion zoning (Type III) but at an incremental cost of higher average enrichment to compensate for increased leakage. Both Type II and III multiplication factors monotonically increase with burnup due to power shifts to the center of the core as

$^{239}\text{Pu}$  preferentially breeds in the lower-enriched center region. Decreased leakage results in net positive reactivity overriding  $^{235}\text{U}$  depletion and FP poisoning. The preliminary core designs have excess reactivity for cycle length of more than 40 EFPYs providing reactivity margin for replacing some FAs with control rod assemblies (CRAs) and reducing reflector width to satisfy vessel diameter of less than 2.4 m. Therefore, Type III is selected as the reference layout for MicroURANUS.

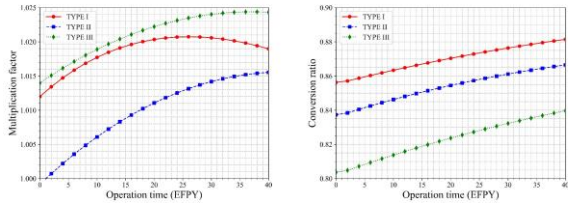


Fig. 3. Evolution of  $k_{eff}$  (left) and conversion ratio (right).

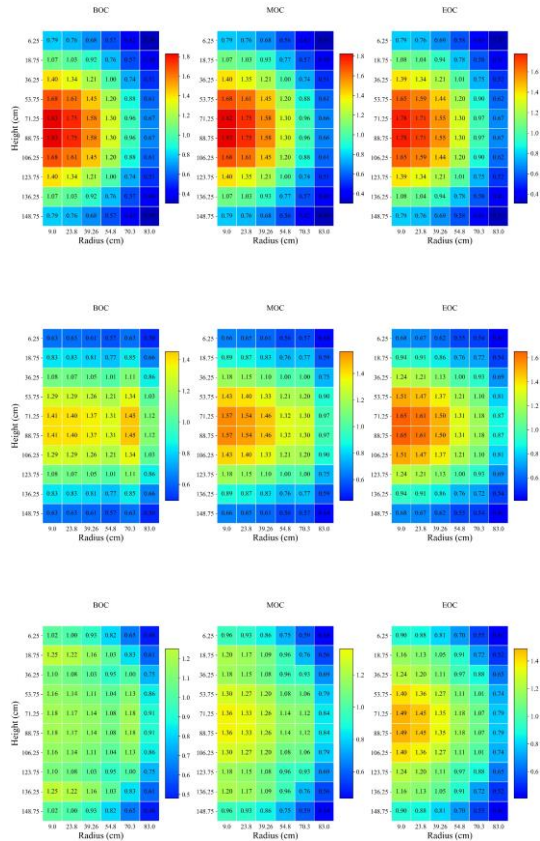


Fig. 4. R-Z power distribution at BOC, MOC, and EOC for Type I, II and III (top to bottom).

### 5. Core performance

The optimized core design adopts an onion zoning core, as shown in Fig. 6. The active core consists of 78 FAs divided into two enrichment zones of 9.75% and 13.6% (adjusted from Type III). Each FA is divided into four axial components: lower reflector, fuel, gas plenum, and

upper reflector. Each axial reflector is 20 cm long and made of stainless steel. The operation fuel temperature is expected to be less than  $900^{\circ}\text{C}$ , and thus the amount of fission gas release is unnoticeable and even negligible. Therefore, the gas plenum length is 10 cm, which might compensate for the gas fission release in MicroURANUS. The CRA system is introduced and divided into two independent systems: the regulating system and shutdown system. The purpose of the regulating system is to regulate the core power during operation, whereas the shutdown system provides a shutdown capability or emergency scram and is fully withdrawn during normal operation. The moderator material ( $\text{ZrH}_{1.6}$ ) is adopted in the CRA to moderate neutrons, which allows an enhanced absorption of the absorber material.  $\text{Gd}_2\text{O}_3$  and  $\text{Eu}_2\text{O}_3$  were selected for the regulating and shutdown CRA, respectively. The main radial reflector material is yttria-stabilized zirconia (YSZ) combined with several LBE coolant channels for heat removal. These are homogenized in the simulation for convenience. The equivalent active core diameter is approximately 170 cm, and the core diameter including the reflector is 200 cm. A barrel of thickness 5 cm is introduced to separate the downcomer coolant from the core zone. The downcomer LBE coolant can be driven in a flow area of thickness 10 cm. The reactor vessel thickness is 5 cm, yielding a reactor vessel outer diameter of 240 cm, which satisfies the requirement for the cavity size of the transportation cask. With these small dimensions, MicroURANUS can be employed as a mobile reactor in nuclear-propelled marine ships. MicroURANUS can achieve a discharged burnup at 30 EFPY of approximately 39 MWd/kgHM with a power density of  $32.7 \text{ W/cm}^3$ .

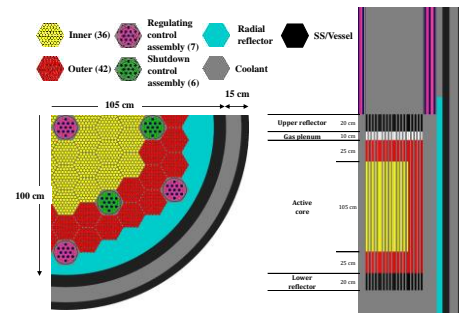


Fig. 5. MicroURANUS radial and axial core layouts.

The neutronic performance of the core in terms of the  $k_{eff}$  behavior and power profiles of the optimized core are investigated in this section. A heterogeneous whole core is simulated using the MC code MCS. The ENDF/B-VII.0 cross-section library is used in MCS. The core  $k_{eff}$  as a function of time with all rods out (ARO) is illustrated in Fig. 6, and it is confirmed that a cycle length of over 30 EFPYs is feasible with a small burnup reactivity swing. Indeed, the average burnup reactivity swing and average delayed neutron fraction over the cycle length correspond to approximately 530 and 724 pcm,

respectively, such that the burnup reactivity swing is less than 1\$ over the full operation time of 30 years.

Figs. 7 and 8 show the normalized radial and axial power profiles with ARO at BOC, MOC, and EOC. The radial assembly power peaks at BOC, MOC, and MOC correspond to 1.063, 1.173, and 1.283, respectively. As shown in these figures, a power peak tends to move from the core periphery at BOC to the core center at EOC. Because of the onion zoning core, the axial power rate is depressed at the interface between the two enrichment zones. Overall, the axial power rate during depletion increases at the core center and decreases at the core bottom and top.

The control rod worth (CRW) and shutdown margin (SDM) are calculated by MCS heterogeneous model (pin by pin) and shown in Tables IV and V. The shutdown system has SDMs at BOC, MOC, and EOC of greater than 2.9\$, which can properly cover the reactivity swing, temperature defect, and other uncertainties during operation.

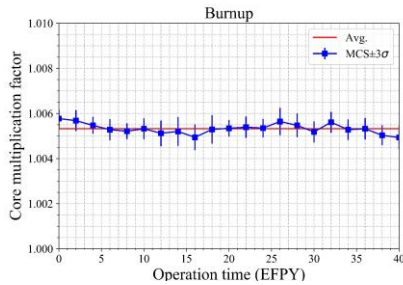


Fig. 6. Evolution of  $k_{eff}$  over operation time.

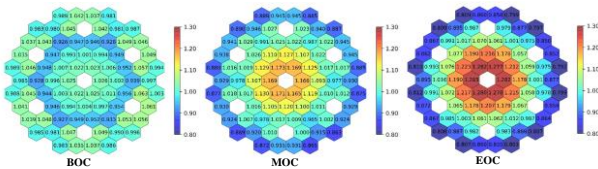


Fig. 7. Radial power distribution.

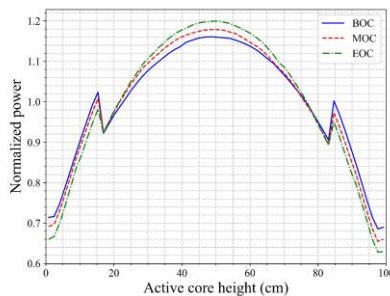


Fig. 8. Core average axial power distribution

Table IV: Control Rod Worth at BOC, MOC, and EOC.

CRW (pcm/\$)	BOC	MOC	EOC
Regulating	3,236±15/ 4.05±0.04	3,085±17/ 4.27±0.06	3,004±15/ 4.58±0.08
Shutdown	7,598±16/ 9.51±0.10	6,836±19/ 9.47±0.13	6,257±14/ 9.54±0.15
Total	11,662±17/ 14.60±0.15	10,735±17/ 14.87±0.20	10,065±17/ 15.35±0.25

Table V: Shutdown Margin (unit: \$)

Parameter	BOC	MOC	EOC
Reactivity changes			
- Excess reactivity swing (ERS, ±0.02)	0.73	0.74	0.76
- Temperature defect HFP → CZP (TD, ±0.03)	0.67	0.65	0.77
Uncertainty at one standard deviation			
- Burnup reactivity swing (15%, ±0.01)	0.11	0.11	0.11
- Temperature defect (20%, ±0.01)	0.13	0.13	0.15
- Others	3.0	3.0	3.0
- Total uncertainties (RSS, ±0.01)	3.24	3.24	3.24
Other margins (OM)	1.8	1.8	1.8
Maximum required worth (MRW = ERS+TD+RSS+OM, ±0.04)	6.44	6.43	6.60
Available reactivity worth (ARW, ±0.13)	9.51	9.47	9.54
Shutdown margin (= ARW – MRW, ±0.13)	3.07	3.04	2.94

## 6. Conclusions

An innovative LMFR core cooled by LBE, MicroURANUS, has been designed to satisfy the requirements of a long-cycle SMR for marine propulsion. The conceptual core has an active equivalent diameter and height of 170 and 155 cm, respectively, and onion enrichment zoning for flattening the power distribution. The outer reactor diameter incorporating the radial reflector, coolant downcomer and primary vessel thickness is 240 cm allowing the entire reactor unit to be factory constructed and transported within a nuclear transportation cask. The MicroURANUS core achieves 30 EFPY operation without refueling or fuel shuffling with less than 1\$ burnup reactivity swing, and the cold fuel design limits reactivity swing from HZP to HFP to be less than 1\$. Several aspects of MicroURANUS in terms of core safety analysis, including the reactivity feedback coefficient and thermal hydraulic at different burnup steps, are to be investigated in the future.

## ACKNOWLEDGEMENT

This work was supported by the National Research Foundation of Korea (NRF) grant funded by the Korea government (MSIT). (No.NRF-2019M2D1A1067205)

## REFERENCES

- [1] Just, L. C., H. Henryson II, A. S. Kennedy, S. D. Sparck, B. J. Toppel, and P. M. Walker. *System aspects and interface data sets of the Argonne Reactor Computation (ARC) System*. No. ANL--7711. Argonne National Lab., 1971.
- [2] Lee, H., W. Kim, P. Zhang, M. Lemaire, A. Khassenov, J. Yu, Y. Jo, J. Park, and D. Lee. "MCS—A Monte Carlo particle transport code for large-scale power reactor analysis." *Annals of Nuclear Energy* 139 (2020): 107276.
- [3] Toshinsky, G. I., A. V. Dedul, O. G. Komlev, A. V. Kondaurov, and V. V. Petrochenko. "Lead-Bismuth and Lead as Coolants for Fast Reactors." *World Journal of Nuclear Science and Technology* 10, no. 02 (2020): 65.
- [4] Cautaerts, N., R. Delville, W. Dietz, and M. Verwerft. "Thermal creep properties of Ti-stabilized DIN 1.4970 (15-15Ti) austenitic stainless steel pressurized cladding tubes." *Journal of Nuclear Materials* 493 (2017): 154-167.